IEEE Access
Multidisciplinary | Rapid Review | Open Access Journal

Received 1 February 2023, accepted 2 March 2023, date of publication 8 March 2023, date of current version 20 March 2023.

Digital Object Identifier 10.1109/ACCESS.2023.3254208

RESEARCH ARTICLE

A Novel Directional Antenna for Next-Generation Fare Payment System

DONG-JIN LEE[1], TAE-KI AN[1], AND IN-JUNE HWANG[2], (Member, IEEE)

[1]Korea Railroad Research Institute, Uiwang, Gyeonggi 16105, South Korea
[2]Electromagnetic Wave Metrology Group, Korea Research Institute of Standards and Science (KRISS), Daejeon 34113, South Korea

Corresponding author: In-June Hwang (injune.hwang@kriss.re.kr)

This work was supported in part by the Research and Development Program through the Development on Interactive Route Guidance and Supporting System Technology for the Mobility Handicapped in Railway Station through the Korea Railroad Research Institute under Grant PK2301C2.

ABSTRACT The fare payment system for public transportation has developed from coins, paper tickets, magnetic strips, and pre-paid cards to new technologies such as Radio-Frequency Identification (RFID) and Near Field Communication (NFC). Most fare payment systems are a fusion of NFC and mobile payment. As the latest fare payment system, the studies on gate-free technology without tag action are in progress. The gate-free system has several advantages, such as improving user convenience, eliminating congestion, and preventing the spread of infectious diseases. We introduce a gate-free system using Bluetooth Low Energy (BLE) technology as the next-generation fare payment system for public transportation. We propose a smart block structure for a gate-free system and analyze the antenna for this structure. A directional antenna is required for location detection of multiple mobile terminals in the gate-free zone, and an antenna to satisfy the requirements is analyzed. A stacked air-gap patch array that satisfies BLE performance and has high directivity has been proposed within the limited smart block size. To compensate for the low bandwidth of the patch antenna, an air gap is added between the patch radiator and the ground, and the antenna gain is increased by applying a stacked patch on the patch radiator. Based on the proposed antenna and smart block, a gate-free system testbed is installed, and the testing results are presented.

INDEX TERMS Directional antenna, fare payment system, gate-free system, smart block.

I. INTRODUCTION

The fare payment system has developed from coins, paper tickets, magnetic strip, and pre-paid card in the past to new technologies such as RFID and NFC, and the emergence of these technologies give a new impetus to innovation in this field. This technology allows us to pay contactless and is becoming a part of consumer habits due to its significant advantages in speed and convenience [1], [2], [3], [4]. As a result, this technology is being used in various places in the industry and public transportation [5], [6]. Currently, most fare payment system for public transportation are a fusion of NFC and mobile payment. In addition, studies on gate-free technology without tag action using face recognition and object tracking are in progress [7], [8].

The associate editor coordinating the review of this manuscript and approving it for publication was Sangsoon Lim.

The railway stations standardized with waiting rooms and platforms have limitations in architectural structure and facilities that inevitably cause congestion through the current physical fare payment system through tagging. By introducing the non-contact fare payment system technology, it is possible to improve the convenience of users moving and transferring, reduce congestion in the bottleneck section around the toll gate and shorten the transfer distance by improving the architectural structure. A gate-free system is one of the non-contact fare payment systems, eliminating toll gates. The gate-free system has an aspect that can ensure safety. The gate-free system can prevent the spread of infectious diseases such as COVID-19 in advance by minimizing contact with facilities and alleviating congestion in the bottleneck area around the toll gates.

The gate-free system applies mobile, beacon, and BLE technologies so that users can automatically pass through

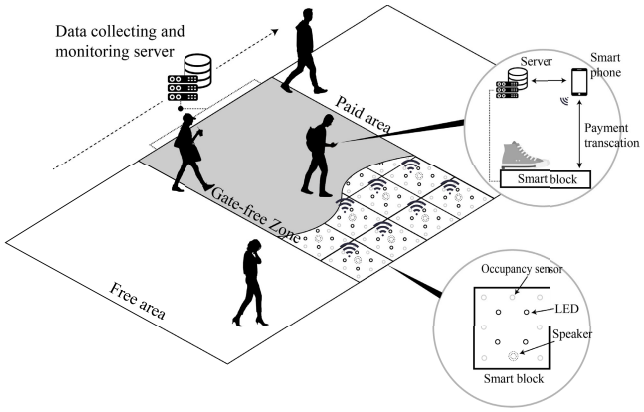

FIGURE 1. Gate-free system configuration.

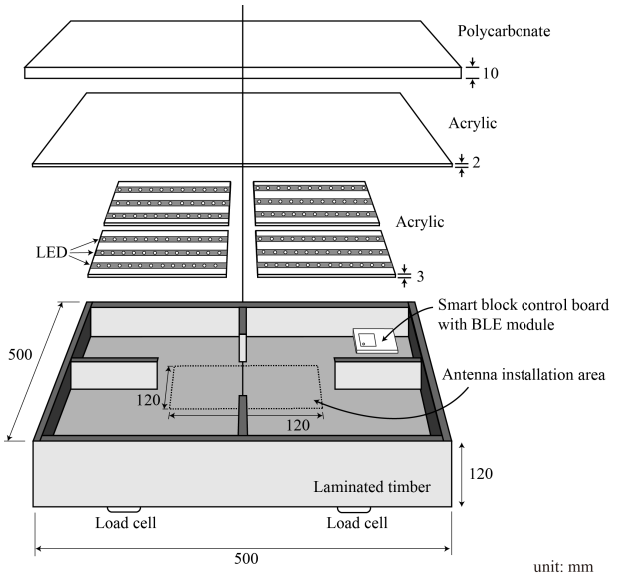

FIGURE 2. Smart block configuration.

when they have a mobile phone with a mobile application installed. The gate-free system consists of a free area, gate-free zone, and paid area, and pedestrians are charged by passing the gate-free zone. The gate-free zone consists of smart blocks, a server that collects and monitors data, and a mobile terminal, as shown in Fig. 1. The smart block of gate free zone consists of an occupancy sensor, LED, speaker, and BLE transmitter. It collects a fare through communication between the terminal and the server after the mobile terminal recognizes the beacon of the BLE transmitter in the smart block. The information is displayed on the smart block with LEDs and speakers to visually and aurally know the illegal ride or payment process.

Terminal location detection technology on the smart block is required for fare collection. The smart block LED and speaker indicate that payment is complete when the fare collection is completed based on location detection. The smart blocks have to recognize the terminal BLE beacon on the corresponding block. In the gate-free system, many passengers pass through the gate-free zone. In the gate-free zone, the smart blocks send a BLE signal to the terminals, and the terminal receives the BLE signal and sends the BLE Received Signal Strength Indication (RSSI) value to the server. In the smart block connected to the server, it is determined that the terminal with the strongest RSSI value is on its own smart block.

When an antenna with an omnidirectional radiation pattern is used, all adjacent smart blocks have similar RSSI values, making it difficult to determine which block the terminal is on. In the case of an antenna having directivity, it is easy to track the position of the terminal because it has a high RSSI value only on the corresponding smart block. However, omnidirectional antennas such as dipole, inverted-F, and helical are used in most existing BLE because it connects arbitrary nearby terminals [9], [10], [11], [12]. When an omnidirectional antenna is used, it is difficult to detect the location of the terminal because all terminals near the smart block are recognized. Accordingly, there is a need for a directional antenna that can precisely detect the location of a terminal on a smart block. As a consequence of their directivity, directional antennas also send less signal from directions other than the main beam. This property reduces interference.

Regarding the study using BLE signals, research on indoor position and Angle Of Arrival (AOA) evaluation is in progress, and most studies estimate position and AOA of BLE beacon from a single scanner [13], [14], [15], [16]. In particular, study on estimating the angle and position by switching multiple antennas is actively underway. Dipole, patch, and ceramic antennas are mainly used in these studies. In the proposed gate-free system, study on an antenna different from the existing BLE antenna is required. The gate free system is a system that distinguishes multiple BLE terminals from multiple transmitters installed on the floor, and it is necessary to study an antenna suitable for this system along with the pressure detection of the load cell.

This paper proposes a directional antenna for location detection of mobile terminals on smart blocks for the proposed gate-free system. We propose a stacked air-gap patch that satisfies BLE performance and has high directivity, considering the smart block structure. The existing patch antenna, which has a low profile, has been widely used due to the advantages of cost, weight, conformability, and ease of manufacturing. The main barrier to using these microstrip patch antennas in many applications is bandwidth [17], [18]. An air gap was added between the patch radiator and the ground to compensate for this low bandwidth. The antenna gain is increased by applying a stacked patch to have the maximum gain in the smart block structure.

II. SMART BLOCK ARCHITECTURE AND DESIGN

The smart block structure for gate-free system is shown in Fig. 2. 10 mm thick polycarbonate and 2 mm thick acrylic are installed on the top plate. Laminated timber is placed under

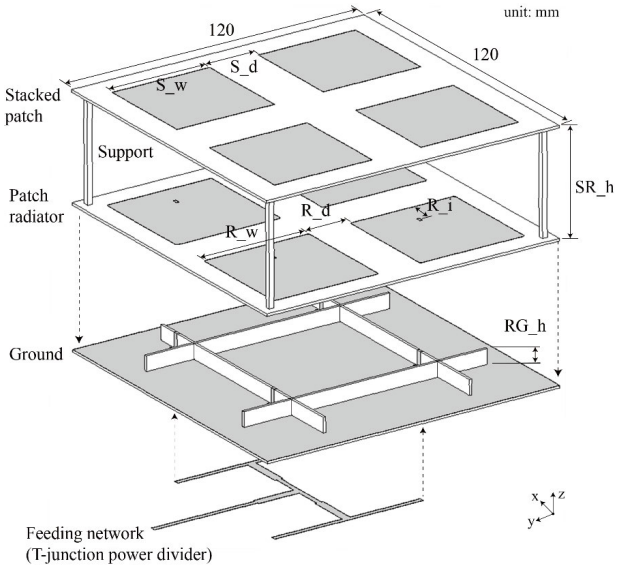

FIGURE 3. Proposed antenna structure.

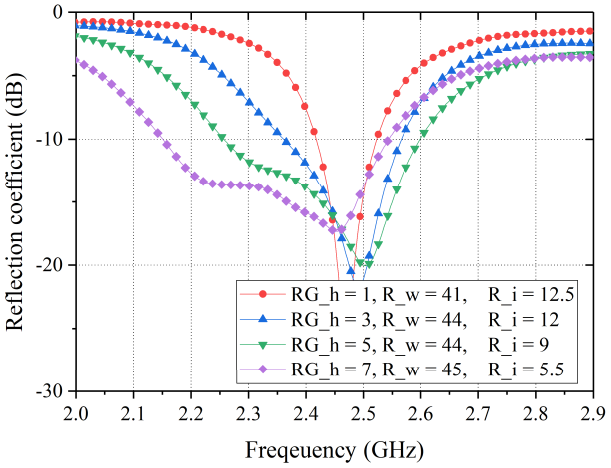

FIGURE 4. Reflection coefficient with variation of *RG_h*.

the 2 mm thick acrylic, and load cell sensors are installed under the timber, so it can be confirmed that a person is on the smart block. Four 2 mm thick acrylic plates and a control board are placed in the laminated timber, and LEDs are attached to the acrylic plate. A BLE module is attached to the control board to communicate with the mobile terminal. The control board controls the load cell, LED and performs communication with the server. The RF terminal of the BLE module is connected to a separate antenna through a cable, and the antenna installation area is shown in Fig. 2. It has a size of 120 mm by 120 mm, and the height is less than 100 mm. It is necessary to design an antenna having high directivity with covering the BLE band of 2.4 - 2.4835 GHz in a limited size. It is also necessary to analyze the effect of the LED on the antenna.

Considering the requirements, we propose a stacked air-gap patch antenna, as shown in Fig. 3. The stacked patch structure is proposed as shown in [19], and it was confirmed that the antenna peak gain can be optimized by using substrates with various dielectric constants and distances. In this paper, we proposed an antenna that satisfies the bandwidth and antenna gain suitable for the specific application by using an FR4 substrate with a single permittivity in a physically limited structure. An antenna structure using an air-gap to satisfy the bandwidth and a stacked patch to increase the gain is analyzed in a physically limited structure of the smart block. The antenna consists of a stacked patch, patch radiator, ground, and feeding network. The 2 × 2 patch array antenna is adopted, which is easy to manufacture in a limited area and has a high gain. In order to compensate for the narrow bandwidth of the patch antenna, an air gap (*RG_h*) is introduced. In addition, the stacked patch with the gap (*SR_h*) is introduced to have higher directivity. The signal feeding to each patch antenna is performed by direct feeding using support between patch radiator and ground. The feeding using support makes it easy to fabricate. The feeding network is made on the underside of the ground using T-junction power dividers.

Fig. 4 shows the bandwidth according to the distance change between the patch radiator and ground (*RG_h*). As *RG_h* increases, the effective dielectric constant of the suspended patch antenna decreases, and patch radiator size (*R_w*) should increase accordingly. As the impedance of the patch antenna decreases, the position of 50-ohm feeding (*R_i*) should decrease. When *RG_h* is 1, 3, 5 and 7, the -10 dB bandwidth is 4.3, 8.4, 14 and 16 %, respectively.

A stacked patch is used to increase the antenna gain as much as possible in the limited area of the smart block. The gain variation according to the stacked patch width (*S_w*) and the distance between the patch radiator and the stacked patch (*SR_h*) are shown in Fig. 5. The antenna gain is measured at the resonant frequency of 2.45 GHz. When *SR_h* is 0.2λ, the antenna gain according to the change of *S_w* is shown in Fig. 5(a). As *S_w* increases up to 40 mm, the gain increases and then decreases. When *S_w* is 40 mm, the gain according to the change of *SR_h* is shown in Fig. 5(b). When *R_h* is 28 mm, it has a peak gain of 12.4 dBi. This result is an increase of 1.8 dB compared to 10.6 dBi without the stacked patch. Considering bandwidth and gain, *S_d*, *R_w*, *R_d* and *R_i* are 20, 44, 16, and 15 mm respectively.

To examine the effect of the LED on the antenna, the effect of the metal on the antenna is analyzed as shown in Fig. 6. Since LED is a semiconductor that emits light according to the flow of current, simulation is performed assuming that it is a metal to simplify modeling. In actual use, it can be used by attaching LEDs on the metal above the proposed antenna. By placing metal on the stacked patch, the antenna impedance and radiation pattern changes are investigated. Fig. 6(a) shows the arrangement of the LED in the orthogonal direction to the antenna polarization, and Fig. 6(b) shows the arrangement of the LED in the direction of the antenna polarization.

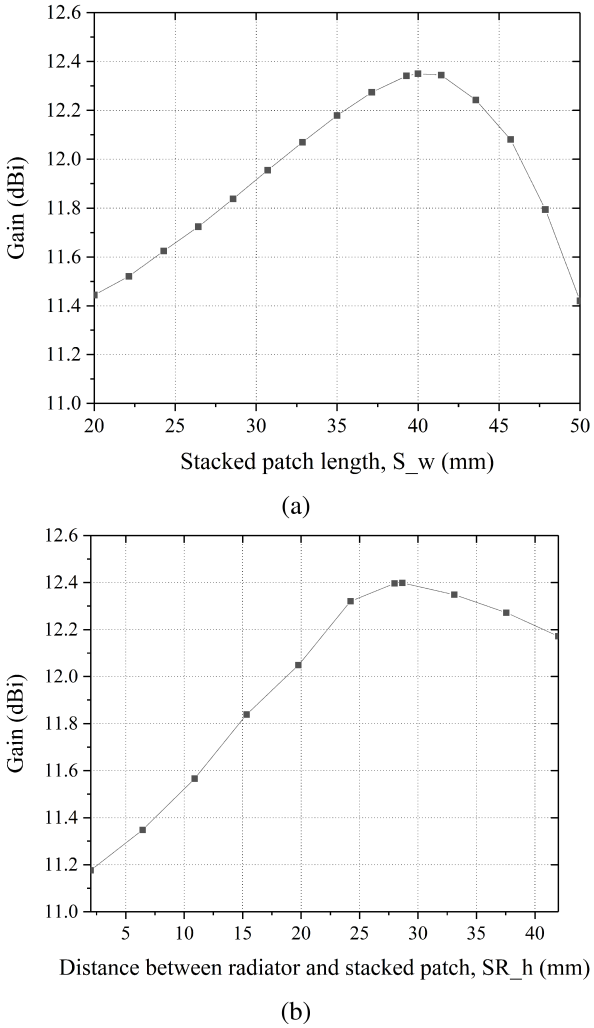

FIGURE 5. Gain with variation of stacked patch parameters: (a) *S_w*, and (b) *SR_h*.

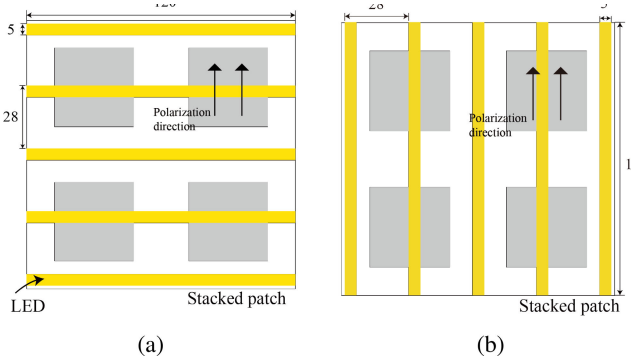

FIGURE 6. Arrangement of the LED on the stacked patch: (a) opposite direction of polarization, and (b) direction of polarization.

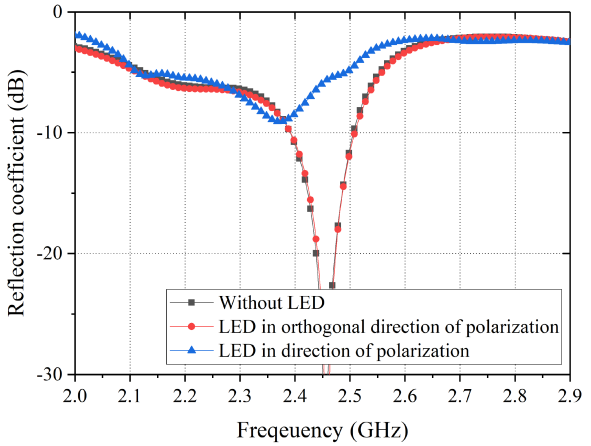

FIGURE 7. Reflection coefficient with LED attachment effect.

Fig. 7 shows the change of the reflection coefficient by the effect of the LED on the antenna. As shown in Fig. 7, LEDs orthogonal to polarization do not affect the antenna impedance, but LEDs in the polarization direction cause changes in antenna impedance, and it can be seen that the S-parameter deviates from the center frequency. The resonant frequency of a patch antenna is determined by the length of the patch, and the impedance is determined by the width of the patch and the feeding point. In the case of metal in the same direction to the polarization, the resonant frequency of the antenna is lowered by making the length of the patch antenna longer, which makes it difficult to radiate at the target frequency. In the case of metal in the opposite direction to the polarization, the width of the patch antenna is increased to affect the impedance, but the change is insignificant compared to the length. Antenna impedance is largely determined by the feeding point. As a result, the reflection coefficient of the antenna is greatly affected in the case of LEDs of the same polarization direction, and the effect is negligible in the case of LEDs of the opposite reflection. It is analyzed that the same principle as above is applied to the stacked patch to affect the antenna performance. It is also confirmed that the LED in the orthogonal direction to the polarization does not affect the radiation pattern of the antenna.

To confirm the identification of the terminal on the smart block, the received power according to the movement of the pedestrian at the height of 1 m above the smart block is compared. The received power with the inverted-F antenna, the single patch antenna, the 2 × 2 patch antenna, and the proposed antenna are compared using the Friis transmission equation. The inverted-F antenna represents a typical PCB BLE antenna. 3D EM simulation results are used for the transmit antenna pattern. The receive antenna gain is 0 dB, and free space between the transmit and receive antennas is assumed. The BLE device is the ESP32 model, which can adjust the BLE power from −12 dBm to +9 dBm. Here, the transmit power is set to −12 dBm. The received power, according to the change of distance from the center of the smart block by the horizontal movement (d), is shown in Fig. 8. The distance from the center of a smart block to the center of the adjacent smart block is 500 mm.

Therefore, the more significant the difference in received power between d = 0mm and 500mm, the easier it is to distinguish terminals on and nearby the smart block. The

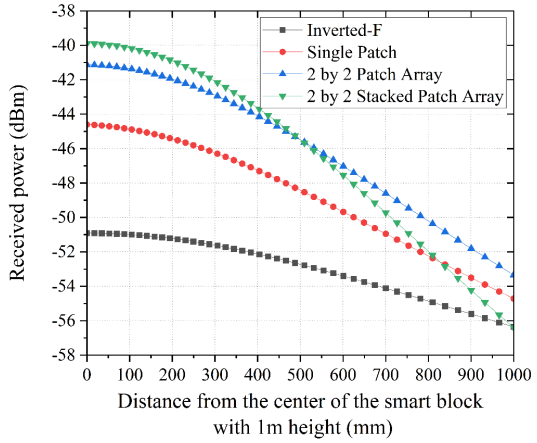

FIGURE 8. Simulated received power according to the distance from the center of the smart block.

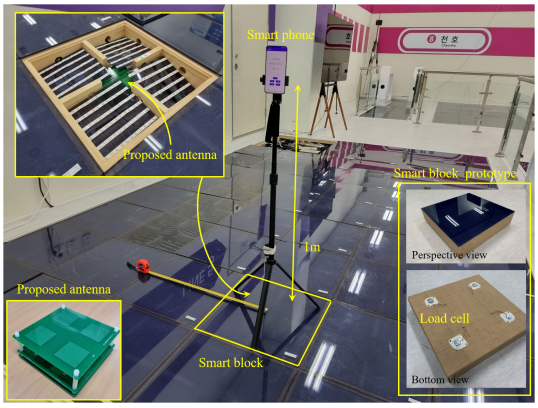

FIGURE 9. Smart block prototype and gate-free system testbed.

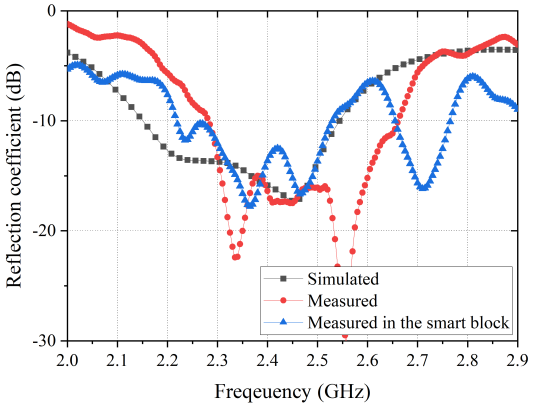

FIGURE 10. Reflection coefficient of the prototype.

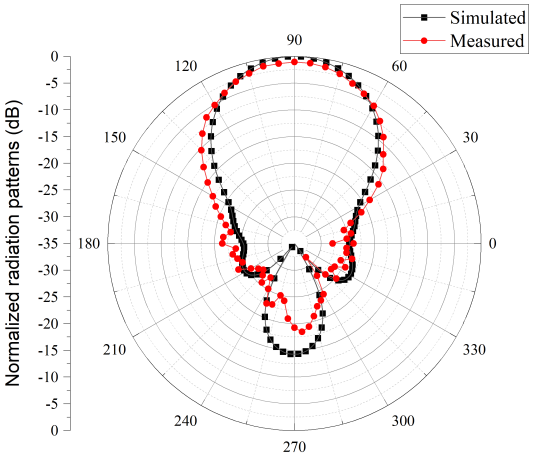

FIGURE 11. Radiation pattern of the prototype.

difference in received power when d is 0 mm, and 500mm is 1.87 dB for inverted-F, 3.93 dB for a single patch, 4.50 dB for 2 × 2 patch antenna, and 5.77 dB for the proposed 2 × 2 stacked patch antenna. The Friis equation does not include the multi-path fading effect, the antenna performance of the receiving terminal, the surrounding environment of the receiving terminal, and the influence of nearby people. In order to reflect a variety of circumstances, it is necessary to detect the terminal through repeated observation while pedestrians pass over multiple smart blocks.

III. SMART BLOCK ANTENNA FABRICATION AND PERFORMANCE RESULTS

The fabricated smart block and gate-free system testbed is shown in Fig. 9. In the testbed, a gate-free zone is constructed with many smart blocks. The perspective view and a bottom view of the smart block prototype is in the bottom right of Fig. 9. The load cell is installed under the smart block to measure pressure. The proposed antenna is placed in the smart block. The smart block also has LEDs, a control board, and a BLE module. The s-parameter of the fabricated prototype is shown in Fig. 10. The -10dB bandwidth is 16 % for simulation, 15.4 % for measurement, 12.7 % for measurement with antenna mounting in the smart block. The difference between the simulated and the measured results is from the change in position and height of the feed point of integral support during the antenna fabrication process. Although the s-parameter in the smart block is reduced due to the influence of wires and control boards, the bandwidth of BLE is still covered. The radiation pattern of the fabricated proposed antenna is similar to that of the simulation, as shown in Fig. 11. The radiation pattern is measured at a center frequency of 2.45 GHz and shows a similar radiation pattern at the BLE operating frequency. The measured peak gain is 11.3 dBi, and the 3dB beamwidth is approximately 50°. Table 1 compares the proposed antenna in a smart block for a gate-free system with a reference antenna of similar physical size. It can be confirmed that the proposed antenna has an appropriate bandwidth and high antenna gain even with a small antenna size.

In order to analyze the performance of the fabricated smart block, the RSSI is measured from a height of 1m in the testbed. BLE signal is transmitted through the antenna of the smart block, and the antenna is inverted-F, single patch, 2 × 2 patch array, and the proposed stacked patch array. The BLE device is the ESP32 model, and the transmission power is set

TABLE 1. Comparing proposed antenna to the previously reported antenna.

Ref.	Type	Volume (λ_0^3)	BW($\|S_{11}\|$ <-10dB)	Max gain (dBi)
[20]	Folded slot	1.8*1.4*0.08	7.4%	13.2
[17]	Modified ring patch	1.17*1.17*0.19	70%	9.2
[21]	Stacked dielectric resonator	1.26*1.26*0.27	40%	10.5
[22]	Stacked patch	1.19*1.19*0.08	19%	11
Proposed	Stacked patch	0.98*0.98*0.57	15%	11.3

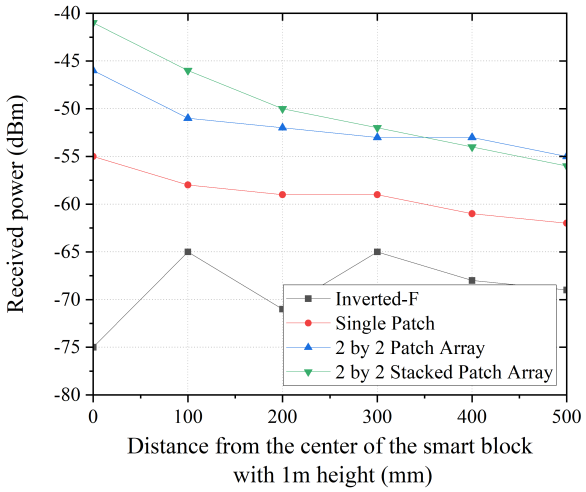

FIGURE 12. Measured received power according to the distance from the center of the smart block.

to -12 dBm. A mobile terminal is installed at the height of 1 m on the smart block, and a Samsung Galaxy S22 is used as the mobile terminal. RSSI at the horizontal distances d of 0, 100, 200, 300, 400, and 500 mm from the center of the block is measured, and the difference in receiving power with a nearby terminal is compared. The results according to the measurement are shown in Fig. 12.

Inverted-F antenna showed RSSI of -65 ∼ -75 dBm regardless of distance, and other antennas showed a tendency to decrease in receiving power as the distance increased. The difference in received power when d is 0 mm, and 500mm is 7 dB for a single patch, 9 dB for 2 × 2 patch antenna, and 15 dB for a proposed 2 × 2 stacked patch antenna. This result shows that the proposed antenna could distinguish a terminal on the corresponding smart block and a nearby terminal more than other antennas. The test result shows a more significant difference than the simulation, and it is judged that the influence of the propagation environment and the mobile terminal is significant. The test results are summarized in Table 2. As shown in Table 2, it is confirmed that the received power difference between the corresponding block and the adjacent block is greater about 6 dB than that of the 2 × 2 array antenna.

TABLE 2. Summary of gate-free system testbed results.

	Inverted-F	Single Patch	2 × 2 Patch array	Proposed 2 × 2 stacked patch array
Corresponding block (d = 0)	-75 dBm	-55 dBm	-46 dBm	-41 dBm
Adjacent block (d = 500)	-69 dBm	-62 dBm	-55 dBm	-56 dBm
Difference	-6 dB	7 dB	9 dB	15 dB

The smart block uses load cells and BLE technology. When multiple passengers with terminals come to the gate-free zone and the passenger steps on a smart block, the smart block must distinguish the terminal above itself using BLE RSSI. A highly directive antenna for the distinction of these terminals is essential. The proposed antenna shows a higher directivity than the existing antenna, reduces transmit to other direction than the main beam to mitigate interference, and creates a larger RSSI difference with a nearby smart block. The performance of the proposed antenna was verified through tests on the testbed. The variation of RSSI is quite large depending on the propagation environment, so there is a limit to tracking, but it is judged that the position can be tracked through supplementation of the software algorithm and repetitive measurement by passing a number of smart blocks.

IV. CONCLUSION

A smart block for a gate-free system and an antenna within a limited smart block are proposed. The proposed antenna is designed to have high directivity to recognize the location of the terminal in the gate-free zone. The proposed antenna and the existing antennas are compared through the gate-free system testbed, and it is confirmed that the proposed antenna performs better in distinguishing adjacent terminals. The proposed antenna and smart block will enable the realization of the gate-free system, creating a novel fare payment system.

REFERENCES

[1] M. G. Gnoni, V. Elia, and A. Rollo, "RFID technology for an intelligent public transport network management," *Int. J. RF Technol.*, vol. 3, no. 1, pp. 1–13, 2012.
[2] M. G. Gnoni, A. Rollo, and P. Tundo, "A smart model for urban ticketing based on RFID applications," in *Proc. IEEE Int. Conf. Ind. Eng. Eng. Manage.*, Dec. 2009, pp. 2353–2357.
[3] M. Burden, "Near field communications (NFC) in public transport," in *Proc. IET Seminar RFID Electron. Vehicle Identificat. Road Transp.*, 2006, pp. 21–38.
[4] R. Widmann, S. Grunberger, B. Stadlmann, and J. Langer, "System integration of NFC ticketing into an existing public transport infrastructure," in *Proc. 4th Int. Workshop Near Field Commun.*, Mar. 2012, pp. 13–18.
[5] K. Finkenzeller, *RFID Handbook: Fundamentals and Applications in Contactless Smart Cards, Radio Frequency Identification and Near-Field Communication*. Hoboken, NJ, USA: Wiley, 2010.
[6] C. Yang and A. P. Sample, "EM-ID: Tag-less identification of electrical devices via electromagnetic emissions," in *Proc. IEEE Int. Conf. RFID (RFID)*, May 2016, pp. 1–8.
[7] V. Coskun, B. Ozdenizci, and K. Ok, "A survey on near field communication (NFC) technology," *Wireless Pers. Commun.*, vol. 71, no. 3, pp. 2259–2294, 2013.

[8] V. Fegade, A. Chodankar, A. Bhingle, and S. Mhatre, "Residential security system based on facial recognition," in *Proc. 6th Int. Conf. Trends Electron. Informat. (ICOEI)*, Apr. 2022, pp. 1–9.
[9] B. S. Yildirim, B. A. Cetiner, G. Roqueta, and L. Jofre, "Integrated Bluetooth and UWB antenna," *IEEE Antennas Wireless Propag. Lett.*, vol. 8, pp. 149–152, 2009.
[10] Y.-F. Liu, P. Wang, and H. Qin, "Compact ACS-fed UWB monopole antenna with extra Bluetooth band," *Electron. Lett.*, vol. 50, no. 18, pp. 1263–1264, 2014.
[11] A. Kumar and P. V. Naidu, "A novel compact printed ACS fed dual-band antenna for Bluetooth/WLAN/WiMAX applications," in *Proc. Prog. Electromagn. Res. Symp. (PIERS)*, Aug. 2016, pp. 2000–2003.
[12] S. K. Mishra, R. K. Gupta, A. Vaidya, and J. Mukherjee, "Printed fork shaped dual band monopole antenna for Bluetooth and UWB applications with 5.5 GHz WLAN band notched characteristics," *Prog. Electromagn. Res. C*, vol. 22, pp. 195–210, 2011.
[13] H. Ye, B. Yang, Z. Long, and C. Dai, "A method of indoor positioning by signal fitting and PDDA algorithm using BLE AOA device," *IEEE Sensors J.*, vol. 22, no. 8, pp. 7877–7887, Apr. 2022.
[14] F. Ye, R. Chen, G. Guo, X. Peng, Z. Liu, and L. Huang, "A low-cost single-anchor solution for indoor positioning using BLE and inertial sensor data," *IEEE Access*, vol. 7, pp. 162439–162453, 2019.
[15] R. Ramirez, C.-Y. Huang, C.-A. Liao, P.-T. Lin, H.-W. Lin, and S.-H. Liang, "A practice of BLE RSSI measurement for indoor positioning," *Sensors*, vol. 21, no. 15, p. 5181, Jul. 2021.
[16] R. Giuliano, G. C. Cardarilli, C. Cesarini, L. Di Nunzio, F. Fallucchi, R. Fazzolari, F. Mazzenga, M. Re, and A. Vizzarri, "Indoor localization system based on Bluetooth low energy for museum applications," *Electronics*, vol. 9, no. 6, p. 1055, Jun. 2020.
[17] M. M. Honari, A. Abdipour, and G. Moradi, "Bandwidth and gain enhancement of an aperture antenna with modified ring patch," *IEEE Antennas Wireless Propag. Lett.*, vol. 10, pp. 1413–1416, 2011.
[18] Y. Chen, S. Yang, and Z. Nie, "Bandwidth enhancement method for low profile E-shaped microstrip patch antennas," *IEEE Trans. Antennas Propag.*, vol. 58, no. 7, pp. 2442–2447, Jul. 2010.
[19] H. Attia, L. Yousefi, and O. Ramahi, "High-gain patch antennas loaded with high characteristic impedance superstrates," *IEEE Antennas Wireless Propag. Lett.*, vol. 10, pp. 858–861, 2011.
[20] Z. Liang, S. Lv, Y. Li, J. Liu, and Y. Long, "Compact folded slot antenna and its endfire arrays with high gain and vertical polarization," *IEEE Antennas Wireless Propag. Lett.*, vol. 19, no. 5, pp. 786–790, May 2020.
[21] Y. M. Pan and S. Y. Zheng, "A low-profile stacked dielectric resonator antenna with high-gain and wide bandwidth," *IEEE Antennas Wireless Propag. Lett.*, vol. 15, pp. 68–71, 2016.
[22] X. Yang, L. Ge, J. Wang, and C.-Y.-D. Sim, "A differentially driven dual-polarized high-gain stacked patch antenna," *IEEE Antennas Wireless Propag. Lett.*, vol. 17, no 7, pp. 1181–1185, Jul. 2018.

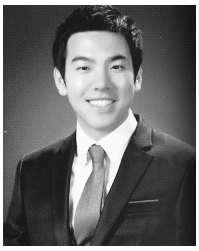

DONG-JIN LEE received the B.S. degree from Korea University, Seoul, South Korea, in 2010, and the Ph.D. degree in electrical engineering from the Korea Advanced Institute of Science and Technology (KAIST), Daejeon, South Korea, in 2017. From 2017 to 2019, he was with the Department of I&C Electrical Engineering, Korea Institute of Nuclear Safety (KINS), Daejeon, where he worked on safety evaluation and EMC verification of I&C equipment of nuclear power plant. He is currently a Senior Researcher with the Korea Railroad Research Institute (KRRI). His research interests include the RF/microwave antenna and system design, wireless power transfer and RF energy transfer/harvesting, and the IoT sensors.

TAE-KI AN received the M.S. degree in electronic engineering from Kyungpook National University, Daegu, South Korea, in 1996, and the Ph.D. degree from the Department of Electrical and Computer Engineering, Sungkyunkwan University, Seoul, South Korea, in 2011. He is a Principal Researcher with the Korea Railroad Research Institute. His research interests include artificial intelligence, pattern recognition, and video analysis.

IN-JUNE HWANG (Member, IEEE) received the B.S. degree in electrical and electronic engineering from Yonsei University, Seoul, South Korea, in 2013, and the M.S. and Ph.D. degrees in electrical engineering from the Korea Advanced Institute of Science and Technology (KAIST), Daejeon, South Korea, in 2015 and 2019, respectively. Since 2019, he has been a Senior Research Scientist with the Division of Physical Metrology, Electromagnetic Wave Metrology Group, Korea Research Institute of Standards and Science (KRISS), Daejeon. His current research interests include electromagnetic field strength, antenna measurement standards, millimeter-wave antennas, phased array antenna systems, energy harvesting, and RF wireless power transfer.